Eur. Phys. J. A **15**, 505–515 (2002)
DOI 10.1140/epja/i2002-10047-3

THE EUROPEAN PHYSICAL JOURNAL A

Explicit model realizing parton-hadron duality

R. Fiore[1,a], A. Flachi[2,b], L.L. Jenkovszky[3,c], A.I. Lengyel[4,d], and V.K. Magas[3,5,e]

[1] Dipartimento di Fisica, Università della Calabria & INFN-Cosenza, I-87036 Arcavacata di Rende, Cosenza, Italy
[2] IFAE, Universidad Autònoma de Barcelona, 08193 Bellaterra, Barcelona, Spain
[3] Bogolyubov Institute for Theoretical Physics, Academy of Sciences of Ukraine, Metrologicheskaya st. 14b, 01143 Kiev, Ukraine
[4] Institute of Electron Physics, Universitetska 21, UA-88000 Uzhgorod, Ukraine
[5] Center for Physics of Fundamental Interactions, Instituto Superior Tecnico, Av. Rovisco Pais, 1049-001 Lisbon, Portugal

Received: 7 June 2002 /
Published online: 10 December 2002 –
Communicated by V.V. Anisovich

Abstract. An explicit model realizing parton-hadron duality and fitting the data is suggested. Complex nonlinear Regge trajectories are important ingredients of the model. The inclusion of Δ and N^* trajectories should account for all resonances in the direct channel. The exotic trajectory is responsible for the smooth background.

PACS. 12.40.Nn Regge theory, duality, absorptive/optical models – 13.60.Hb Total and inclusive cross-sections (including deep-inelastic processes)

1 Introduction

The photoabsorption cross-section in the resonance region has been studied in a large number of papers [1–5] (for a comprehensive review see ref. [6]). There are nearly 20 resonances in the $\gamma^* p$ system in the region between the pion-nucleon threshold and below 2 GeV, but only a few of them can be identified more or less unambiguously. One reason is that they overlap and compete with changing Q^2 and the other is the uncertainty due to the background. Therefore, instead of identifying each resonance, one considers three maxima above the elastic-scattering peak, corresponding to some "effective" resonance contributions. Most of the data come from SLAC and have been compiled by Stoler [7]. The first maximum is due to the isolated $\Delta(1232)$-resonance. The second resonance region is dominated by two strong negative-parity states, the $D_{13}(1520)$ and the $S_{11}(1535)$. At low Q^2 (< 1 GeV^2) the $D_{13}(1520)$ dominates, whereas at high Q^2 (~ 3 GeV^2) there is some evidence that the $S_{11}(1535)$ becomes dominant. The relative strength of the other states is not well determined, especially at increasing Q^2. For example, in the fits for $Q^2 > 4$ GeV^2 it is usually assumed that only $S_{11}(1535)$ contributes to the second resonance, eventually corrected for $Q^2 \leq 4$ GeV^2 to subtract the contribution from the $D_{13}(1520)$. In the third resonance region, the strongest excitation at low Q^2 is the $F_{15}(1680)$ state. Although it is assumed that this remains one state, it is possible that several states contribute strongly at high Q^2. All the fits include a state at $W = 1440$ MeV, corresponding to the possible location of the $P_{11}(1440)$, but these fits do not exhibit any positive contribution from this state. Ultimately, in most of the phenomenological fits only three peaks are included, namely those at $W \sim 1232$, 1535 and 1680 MeV.

The standard approach to the phenomenological analysis of the data is that developed in ref. [1] and still widely used. Ignoring the (relatively small) longitudinal component of the total cross-section, one writes the contribution of the three prominent resonances, $\sigma_{\rm T}^{\rm R} = \sigma_{\rm T}^{\Delta} + \sigma_{\rm T}^{2} + \sigma_{\rm T}^{3}$, with a relativistic Breit-Wigner formula for the Δ-resonance and nonrelativistic formulae for the the second and the third resonance regions[1].

The above resonance contribution is appended by a smooth background, parameterized as

$$\sigma_{\rm T}^{\rm bg} = \sum_{n=1}^{3} C_n(Q^2)(W - W_{\rm th})^{n-1/2}, \qquad (1)$$

[a] e-mail: fiore@cs.infn.it
[b] e-mail: flachi@ifae.es
[c] e-mail: jenk@gluk.org
[d] e-mail: sasha@len.uzhgorod.ua
[e] e-mail: vladimir@cfif.ist.utl.pt

[1] We remind that this is a phenomenological description since the Breit-Wigner formulae are applied to a peak created by a superposition of resonances rather than to a single resonance.

where the square-root term $(W - W_{\rm th})^{1/2}$ takes into account the behaviour of nonresonant pion production at the threshold $W_{\rm th} = m_p + m_\pi$ (m_p is a proton mass). The coefficients $C_n(Q^2)$ are polynomials of Q^2: $C_n(Q^2) = \sum_{j=0}^{4} C_{\rm nj} Q^{2j}$. A detailed analysis of the SLAC data along these lines can be found, *e.g.*, in [4,8].

Systematic theoretical studies of the subject, including the helicity structure of the amplitude, the threshold- and the QCD-motivated asymptotic behaviour of the form factors can be found in the papers by Carlson and coauthors [9,10] (see also ref. [11]). Spin structure functions (SFs) were studied in ref. [12].

Recent results from JLab (CEBAF) [13] renewed the interest in the subject [14–16] and they call for a more detailed phenomenological analysis of the data and a better understanding of the underlying dynamics.

In the present paper we develop further the arguments presented in refs. [17–19] and earlier works cited therein. The basic idea in our approach is to use the off-mass shell continuation of the dual amplitude with nonlinear complex Regge trajectories. These trajectories play a crucial role in the dynamics of the strong interactions. Actually, the trajectories can be considered as the basic dynamical variables, replacing the usual Mandelstam variables s, t and u. In particular, their form determines completely the spectrum of resonances (see, *e.g.*, ref. [20]). The parameters of the trajectories can be fitted independently of the masses and widths of the known resonances, therefore, in principle, they reflect more adequately the position of the peaks in ep scattering, formed by the interplay of different resonances. In concentrating on this aspect of the dynamics, we leave more freedom to the choice of the Q^2-dependent form factors. We start with a simplified model, disregarding the helicity structure of the amplitudes. We ignore the relatively small (and poorly known) contribution from the cross-sections involving longitudinally polarized photons, $\sigma_{\rm L}$. In doing so, we anticipate the connection [17] with the small-x (high-energy) domain, where these simplifications are commonly accepted.

Apart from the above-mentioned details, there is an important problem in the Q^2-dependence, namely the asymptotic behaviour of the form factors, usually related to the quark counting rules. While the validity of these rules for elastic form factors leaves a little doubt, they may get modified for the transition form factors. Moreover, in our approach a new type of form factors, generalizing the concept of inelastic form factors, appears. These new form factors correspond to the transition of the nucleon to a baryon trajectory, with a sequence of nucleon resonances on it. It follows from dual models (see sect. 3 and ref. [17]) that the powers of these form factors increase with the spin of the excited state.

We adopt the two-component picture of strong interactions [21], according to which direct-channel resonances are dual to cross-channel Regge exchanges and the smooth background in the s-channel is dual to the Pomeron exchange in the t-channel. As explained in ref. [17], the background corresponds in a dual model to a pole term with an exotic trajectory that does not produce any resonance.

To summarize the philosophy of the present paper (for a related approach see ref. [22]), we believe that the mechanism of virtual photoproduction on nucleons is not much different from that in purely hadronic processes. Since at intermediate energies the entire nondiffractive part of the hadronic amplitude is saturated by direct-channel resonances, by duality they determine completely the dynamics of the reaction. By expressing the inelastic electron scattering cross-section through the imaginary part of the virtual Compton scattering amplitude, it is reasonable to assume that a resonance model will work for virtual Compton scattering equally well as for pion-nucleon scattering, *i.e.* both are saturated by the contribution of many overlapping resonances. The crucial problem is the spectrum of these resonances, connected with the form of nonlinear, complex Regge trajectories.

The paper is organized as follows: the kinematics of eN scattering and the relevant notations are described in sect. 2. The properties of Regge trajectories, which constitute a basic ingredient of our model, are discussed in sect. 3. The model for the nucleon structure function is presented in sect. 4 and the fitting procedure and comparison with data is discussed in sect. 5. Sections 6 and 7 are devoted to analytical and numerical tests of parton-hadron duality. Finally, we draw our conclusions in sect. 8.

2 Notation, kinematics and observables

We study the inclusive electron-nucleon scattering shown in fig. 1. The scattered electron entering the process with energy E emerges with energy E' at the angle θ with respect to the initial direction. The four-momentum transferred by the virtual photon from the electron to the nucleon is $q = k - k' = -Q^2$, where k and k' are the four-momenta of incoming and outgoing electrons, respectively. The energy transferred between the electron and the nucleon (or the energy lost by the electron) is

$$\nu = \frac{pq}{m} = E - E', \tag{2}$$

where p is the four-momentum of the target nucleon of mass m. The invariant squared mass of the recoiling system (hadronic final state) is

$$W^2 = (p+q)^2 = m^2 + 2m\nu - Q^2. \tag{3}$$

For the reaction $e(k)+N(p) \to e'(k')+X$, the quantity measured in the experiment is the differential cross-section (see, *e.g.*, ref. [23])

$$\frac{{\rm d}^2\sigma^{\gamma^* p}}{{\rm d}\Omega {\rm d}E'} = \Gamma(\sigma_{\rm T} + \epsilon\sigma_{\rm L}), \tag{4}$$

where

$$\Gamma = \frac{\alpha K}{2\pi^2 Q^2} \frac{E'}{E} \frac{1}{1-\epsilon}, \tag{5}$$

with $K = (W^2 - m^2)/(2m)$ and

$$\epsilon = \left(1 + 2\frac{\nu^2 + Q^2}{Q^2} \tan^2\frac{\theta}{2}\right)^{-1}, \tag{6}$$

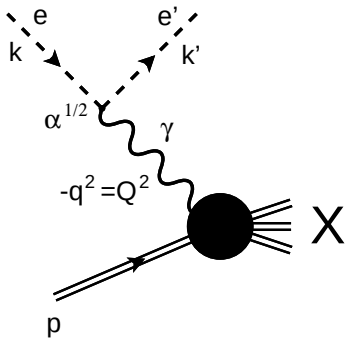

Fig. 1. Kinematics of deep-inelastic scattering.

or

$$\frac{\mathrm{d}^2\sigma^{\gamma^* p}}{\mathrm{d}\Omega \mathrm{d}E'} = \Gamma \sigma_{\mathrm{T}}(1+\epsilon R). \tag{7}$$

The ratio $R = \sigma_{\mathrm{L}}/\sigma_{\mathrm{T}}$ relates the transverse component of the cross-section, σ_{T}, to the longitudinal component, σ_{L}. The structure function F_2 can be expressed in terms of the differential cross-section and R as

$$F_2 = \frac{\mathrm{d}^2\sigma^{\gamma^* p}}{\mathrm{d}\Omega \mathrm{d}E'} \frac{1+R}{1+\epsilon R} \left[\frac{K\nu}{4\pi^2\alpha} \frac{1}{\Gamma} \frac{1}{1+\frac{\nu^2}{Q^2}} \right] , \tag{8}$$

where the kinematics is given by the term in square brackets.

Phenomenological parameterizations for the quantity R exist in the literature [5], but in this paper, as we are ignoring the spin structure, we put $R = 0$.

The central object of the present study is the nucleon SF, uniquely related to the photoproduction cross-section by

$$F_2(x,Q^2) = \frac{Q^2(1-x)}{4\pi\alpha \left(1+\frac{4m^2x^2}{Q^2}\right)} \sigma_{\mathrm{t}}^{\gamma^* p}(s,Q^2) , \tag{9}$$

where the total cross-section, $\sigma_{\mathrm{t}}^{\gamma^* p}$, is the imaginary part of the forward Compton scattering amplitude, $A(s,Q^2)$,

$$\sigma_{\mathrm{t}}^{\gamma^* p}(s) = \mathcal{I}m\ A(s,Q^2) . \tag{10}$$

The centre-of-mass energy of the $\gamma^* p$ system, the negative photon virtuality squared, Q^2, and the Bjorken variable x are related to each other as follows:

$$s = W^2 = Q^2 \frac{(1-x)}{x} + m^2, \tag{11}$$

Instead of W^2, we use the Mandelstam variable s, typical for hadronic reactions.

3 Nonlinear complex Regge trajectories. Direct-channel resonances and background

The SF is related via eq. (9) to the total cross-section, or the imaginary part of the forward Compton scattering amplitude, eq. (10). The latter, on the other hand, is related by unitarity to the sum of all possible intermediate states, as shown in fig. 2 (see, *e.g.*, ref. [24]). One should distinguish between cross-sections summed over a limited number of nuclear excitations [1,7], $\sigma_{\gamma N \to R_i}$ and the total cross-section of the virtual forward Compton scattering, related to the SF, including by unitarity all possible intermediate states allowed by energy and quantum-number conservation.

The correct way to account for all possible intermediate states in the resonance region can be done in terms of the s-channel Regge trajectories, which automatically include the huge number of resonances as recurrences, appearing on the trajectories [19]. This is an economic way to take into account the whole sequence of nucleon excitations, lying on a single trajectory. This is more than a mere technical simplification: Regge trajectories are basic building blocks in dual models. The kinematical variables enter through Regge trajectories, which thus play the role of dynamical variables. Now, since the behaviour of the Regge trajectories is assumed to be known in the whole range of their variation, the resulting behaviour of the SF can be thus extrapolated towards small x, well beyond the resonance region.

The dynamics of the resonance formation is closely related to the form of Regge trajectories. Their linear rise is a widely accepted approximation. It is based on the observed spectrum of resonance masses and was supported by narrow resonance dual models and their mechanical analogues, such as the harmonic oscillator or relativistic strings.

In fact, linear trajectories contradict both the theory and the data: analyticity requires the presence of threshold singularities in the trajectories, while their asymptotic behaviour is also constrained by an upper bound on their real part. The finite widths of resonances also require the presence of a nonvanishing imaginary part in the trajectories.

Explicit models of Regge trajectories realizing the above requirements were studied in a number of papers (see ref. [20,25] and references therein). The main feature of these trajectories is that the number of resonances is finite (due to an upper limit on their real part, determined by fits to the data), as illustrated in fig. 3. A particularly simple model is based on a sum of square roots

$$\alpha(s) = \alpha_0 + \sum_i \gamma_i \sqrt{s_i - s}, \tag{12}$$

where the lightest threshold gives rise to the imaginary part while the heaviest one promotes the nearly linear rise of the real part at small and intermediate s. To simplify the calculations, in a limited range of s, the heaviest threshold can be approximated by a linear term, hence the expression (12) for the trajectory can be written as

$$\alpha(s) = \alpha_0 + \alpha_1 s + \alpha_2(\sqrt{s_0} - \sqrt{s_0 - s}), \tag{13}$$

where s_0 is the lightest threshold, $s_0 = (m_\pi + m_p)^2 = 1.14\,\mathrm{GeV}^2$ in our case. Beyond the threshold, the real part

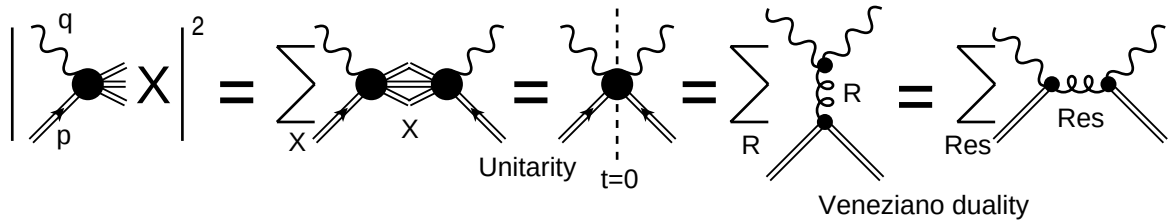

Fig. 2. According to the Veneziano (or resonance-Reggeon) duality a proper sum of either t-channel or s-channel resonance exchanges accounts for the whole amplitude.

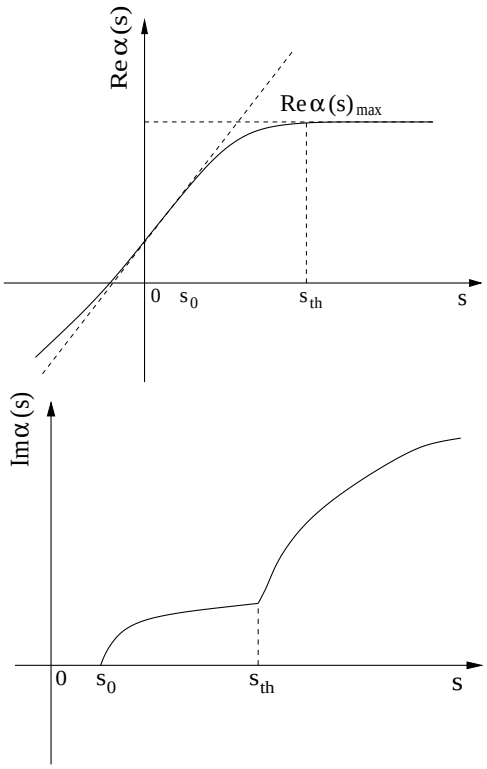

Fig. 3. Typical behaviour of the real and imaginary parts of the analytical model of the Regge trajectory [26]. The (nearly) smooth behaviour results from the smearing of several additive thresholds in eq. (12).

of this trajectory is $\mathcal{R}e\ \alpha(s) = \alpha_0 + \alpha_2\sqrt{s_0} + \alpha_1 s$, while its imaginary part is $\mathcal{I}m\ \alpha(s) = \alpha_2\sqrt{s - s_0}$.

Large-angle scaling behaviour of the hadronic amplitudes constrains [27] the asymptotic (far away from the resonance region) behaviour of the trajectories by a logarithm.

In the $\gamma^* p$ scattering, only N (isospin 1/2) and Δ (isospin 3/2) resonances contribute in the s-channel. The latest Review of Particle Physics [28] quotes about 14 N's whose "existence is certain or very likely certain" (plus 8 N's whose "evidence is fair or poor") and 10 "certain or likely certain" (plus 12 "fair or poor") Δ's. Most, if not all of the above two dozen (almost) certain resonances —among them the "prominent" ones mentioned in the introduction— contribute, with different weights, to the the $\gamma^* N$ total cross-section or to the nucleon SF. It is clear that a systematic account for all these resonances (plus those to be confirmed) is not an easy task. A much more economic way is to introduce the whole sequence of recurrences. As well as generalizing the concept of a resonance (a Regge trajectory realizes the analytical continuation of the discrete resonance spin and is an indispensable ingredient of dual models!), the trajectory may also be used to classify the resonances by eliminating some candidates and predicting others. The above resonances lie on several positive- and negative-parity N and Δ trajectories.

The classification of meson and baryon resonances on the basis of Regge recurrences of $SU(3)$ multiplets was extensively studied in the late sixties (see, *e.g.*, ref. [24]). A nontrivial model for meson Regge trajectories with the limited real part was suggested in a recent paper [20]. Anticipating analogous new results for baryon trajectories, below we shall use a simple model, based on the ideas introduced above and fitted to the three "prominent" resonances, seen in the ep scattering.

4 The model

To illustrate these ideas, we start with a simplified model, in which we disregard the helicity structure of the scattering amplitude and relevant selection rules, concentrating on the role of the Regge trajectories, analyticity and duality. Their role was treated in a number of papers [9] (recently in ref. [29]).

In the dual-Regge approach [17–19] the Compton scattering can be viewed as an off-mass shell continuation of a hadronic reaction, dominated in the resonance region by nonstrange (N and Δ) baryon trajectories. The scattering amplitude follows from the pole decomposition of the dual amplitude [17]

$$A(s,Q^2)\Big|_{t=0} = \text{norm} \sum_{i=N_1^*,N_2^*,\Delta,E} A_i \times \sum_{n=n_i^{\min}}^{n_i^{\max}} \frac{f_i(Q^2)^{2\left(n-n_i^{\min}+1\right)}}{n-\alpha_i(s)}\ , \qquad (14)$$

where i runs over all the trajectories allowed by quantum-number exchange, norm and A_i's are constants, $f_i(Q^2)$'s are the form factors. These form factors generalize the concept of inelastic (transition) form factors to the case of continuous spin, represented by the direct-channel trajectories. The $n_i^{\min}$ refers to the spin of the first resonance

on the corresponding trajectory i (it is convenient to shift the trajectories by 1/2, therefore we use $\alpha_i = \alpha_i^{\rm phys} - 1/2$, which due to the semi-integer values of the baryon spin keeps n in eq. (14) integer). The sum over n goes with step 2 (in order to conserve parity).

It follows from eq. (14) that:

$$\mathcal{I}m\ A(s,Q^2) = \mathrm{norm} \sum_{i=N_1^*,N_2^*,\Delta,E} A_i \times \sum_{n=n_i^{\min}}^{n_i^{\max}} \frac{[f_i(Q^2)]^{2\left(n-n_i^{\min}+1\right)} \mathcal{I}m\ \alpha_i(s)}{(n-\mathcal{R}e\ \alpha_i(s))^2 + (\mathcal{I}m\ \alpha_i(s))^2} \ . \quad (15)$$

Equations (14),(15) have a factorized form, a product of vertices (two identical form factors) times the propagator. Each term in eq. (15) resembles that of a Breit-Wigner formula with a resonance mass $s_n = (n-\alpha_0-\alpha_2\sqrt{s_0})/\alpha_1$ ($\mathcal{R}e\ \alpha(s_n) = n$) and an energy-dependent width given by $\mathcal{I}m\ \alpha(s_n)/\alpha_1$ of the trajectory. The factor $(n-\alpha(s))^{-1}$ is typical of the dual-Regge approach [17].

The first three terms in (15) are the nonsinglet, or Reggeon, contributions with the N^* and Δ trajectories in the s-channel, dual to the exchange of an effective bosonic trajectory (mainly f) in the t-channel, and the fourth term is the contribution from the smooth background modeled by the nonresonance pole term with the exotic trajectory $\alpha_E(s)$, which is dual to the Pomeron (see ref. [17]). As was argued in ref. [17], only a limited number, $\mathcal{N}$, of resonances appears on the trajectories, for that reason we tentatively set $\mathcal{N} = 3$, *i.e.* one resonance on each of the trajectories (N_1^*, N_2^*, Δ). We tried also higher values of $\mathcal{N}$, up to $\mathcal{N} = 10$, but our analysis shows that $\mathcal{N} = 3$ is a reasonable approximation —even if additional peaks appear, they are suppressed as compared to the dominant one (first on each trajectory) due to the Q^2-behaviour of the form factors. Thus, the limited (small) number of resonances contributing to the cross-section follows not only from the location of resonances on a trajectory but also from a strong suppression associated with the behaviour of the numerator (increasing powers of the form factors).

Since, by definition, the smooth background does not show any resonance, here we keep only one term in the sum (for more detail see [17–19] and references therein).

By inserting relevant baryonic trajectories in eq. (15), we include all possible electromagnetic transitions from a nucleon to its excitations. There are, however, selection rules, enhancing some and suppressing others. This effect will be taken into account by our phenomenological fits to the data.

As discussed above the nonlinear behaviour of the trajectories, especially the boundedness of their real part, is a crucial feature of our dual model. For practical reasons we have replaced the formal condition $\mathcal{R}e\ \alpha(s) <$ const by a finite sum in eq. (15), introducing a linear term in the baryon trajectory to approximate the contribution from heavy thresholds (see eq. (13)).

We have fitted to the parameters of baryon trajectories given by eq. (13) in order to reproduce experimental masses and widths of the following resonances:

Resonance	$I\ (J^P)$	M, GeV	Γ, GeV
$\Delta(1236)$	$\frac{3}{2}\left(\frac{3}{2}^+\right)$	1.230	0.115
$N^*(1520)$	$\frac{1}{2}\left(\frac{3}{2}^-\right)$	1.515	0.11
$N^*(1680)$	$\frac{1}{2}\left(\frac{5}{2}^+\right)$	1.690	0.12

We end up with the following trajectories:

$$\alpha_{N_1^*}(s) = -0.8377 + 0.95s + 0.1473(\sqrt{s_0} - \sqrt{s_0 - s}) \ , \quad (16)$$

$$\alpha_{N_2^*}(s) = -0.37 + 0.95s + 0.1471(\sqrt{s_0} - \sqrt{s_0 - s}) \ , \quad (17)$$

$$\alpha_{\Delta}(s) = 0.0038 + 0.85s + 0.1969(\sqrt{s_0} - \sqrt{s_0 - s}) \ . \quad (18)$$

We take only one resonance on each trajectory, so the sum over n in eq. (15) reduces to one term, *i.e.*, $n_i^{\max} = n_i^{\min}$ for all three baryon trajectories as well as for the exotic one.

We take the exotic trajectory in the form

$$\alpha_E(s) = \alpha_E(0) + \alpha_{1E}(\sqrt{s_E} - \sqrt{s_E - s}), \quad (19)$$

where the intercept $\alpha_E(0)$, α_{1E} and the effective exotic threshold s_E are free parameters. As a first approximation we can assume the following expression for the exotic trajectory [17]:

$$\alpha_E(s) = 0.5 + 0.12(\sqrt{s_E} - \sqrt{s_E - s}) \ , \quad (20)$$

where $s_E = 1.145^2$ GeV^2. As was said above, we take only one term from the exotic trajectory. The value $n_E^{\min}$ is the first integer that is larger than Max($\mathcal{R}e\ \alpha_E$) (to be sure that there is no resonance on the exotic trajectory); in our case $n_E^{\min} = 1$.

In dual models, the numerator in eq. (15) contains the powers of the intercepts of the t-channel trajectories, $\alpha_t^n(0)$ and/or the powers of the parameter g that in ref. [17] was assumed to be Q^2-dependent by matching the Regge behaviour and Bjorken scaling. As was mentioned before, here we invert the problem and, in accordance with the factorization properties of the amplitude, we multiply the resonance propagators by the product of the inelastic form factors (to be later identified with the parameters of the dual model [17]).

To start with we use the simplest, dipole model for the form factors, disregarding the spin structure of the amplitude and the difference between electric and magnetic form factors

$$f_i(Q^2) = \frac{1}{\left(1 + \frac{Q^2}{Q_{0,i}^2}\right)^2} \ , \quad (21)$$

where $Q_{0,i}^2$ are scaling parameters.

By considering eq. (15), one can immediately guess that with the increase of Q^2 the first resonance on each trajectory, Δ, N_1^*, N_2^* or E, starts to dominate over subsequent ones, due to the power behaviour of the form factors. The relative growth of these three terms depends on the scaling factor $Q_{0,i}^2$. Therefore, we choose $Q_{0,E}^2 > Q_{0,N_2^*}^2 > Q_{0,N_1^*}^2 > Q_{0,\Delta}^2$ in order to satisfy the

experimentally observed behaviour of these terms, for example, the rise of the background contribution with respect to the resonance one with increasing Q^2; the relative growth of the N_1^* and N_2^* peaks with respect to the Δ peak.

5 Fits to the SLAC and JLab data

In this section we present numerical analysis of our model based on the experimental data from SLAC [7] and JLAB [30][2].

Before displaying the results of our fits, it is instructive to illustrate the ideas behind our study, in order to make the following results more transparent physically.

We are dealing with a set of 704 experimental points for seven different values of Q^2: 0.45, 0.85, 1.4, 1.7, 2.4, 3.0, 3.3 GeV^2. The first rough fit, when the whole data set is taken into account, produces $\chi^2_{\text{d.o.f.}} \propto 10^4$. This has to do with the fact that the set of experimental data is not homogeneous, *i.e.* the points at low s (high x) are given with very small experimental errors, thus "weighting" the fitting procedure not uniformly. This forced us to make a pre-selection in the initial data set by removing the points with $\chi^2_{\text{red}} \leq 1000$. Below we will be considering the leftover of 634 data points (90% of the original data-set), although all the experimental points are presented in figures.

As we have seen in sect. 4, our model consists of the sum of the contributions from three resonances (N_1^*, N_2^*, Δ), which give the dominant contribution to the structure functions, plus an exotic background, that we treat effectively. The first approach to the fitting procedure consists in fixing parameters of the trajectories for the resonances, in order to reproduce the correct masses and widths, leaving the four scaling constants $Q^2_{0,i}$, four factors A_i and the parameters of the exotic trajectories to be fitted to the data. The results are shown in table 1 (third column) and the plots of the SF against x are presented in fig. 4 (dash-dotted lines).

Although the agreement with the experimental data does not seem to be good ($\chi^2_{\text{red}} = 28.29$), there is a number of features which we could introduce in order to improve the model.

The first important step is to account for a larger number of resonances (about 20) available in the energy range under investigation, which overlap, as is noted in sect. 3. For this reason we consider the dominant resonances (N_1^*, N_2^* and Δ) as an "effective" contribution to the SF. In other words, we require that they mimic the contribution of the dominant resonances plus a number of subleading contributions, which together describe completely the real physical system.

In this way we consider corrections to the model as explained in the following. Denoting the structure function as $F(\alpha, x, Q^2)$, where α represents generically the trajectory parameters, the contribution from the subleading resonances can be introduced as corrections to the α's.

[2] We are grateful to M.I. Niculescu for making her data compilation available to us.

Table 1. Parameters of the fit. In the third column we show the result of the fit when the parameters of the baryonic trajectories are fixed. The fourth column contains the result of the fit when the parameters of the trajectories are varied.

N_1^*	α_0	-0.8377 (fixed)[(a)]	-0.8070
	α_1	0.95 (fixed)[(a)]	0.9632
	α_2	0.1473 (fixed)[(a)]	0.1387
	$A_{N_1^*}$	1 (fixed)[(b)]	1 (fixed)[(b)]
	Q^2_{0,N_1^*}, GeV^2	2.4617	2.6066
N_2^*	α_0	-0.37(fixed)[(a)]	-0.3640
	α_1	0.95 (fixed)[(a)]	0.9531
	α_2	0.1471 (fixed)[(a)]	0.1239
	$A_{N_2^*}$	0.5399	0.6086
	Q^2_{0,N_2^*}, GeV^2	2.4617	2.6066
Δ	α_0	0.0038 (fixed)[(a)]	-0.0065
	α_1	0.85 (fixed)[(a)]	0.8355
	α_2	0.1969 (fixed)[(a)]	0.2320
	A_Δ	4.2225	4.7279
	$Q^2_{0,\Delta}$, GeV^2	1.5722	1.4828
	s_0, GeV^2	1.14 (fixed)[(a)]	1.2871
E	α_0	0.5645	0.5484
	α_2	0.1126	0.1373
	s_E, GeV^2	1.3086	1.3139
	A_E	19.2694	14.7267
	Q^2_E, GeV^2	4.5259	4.6041
	norm	0.021	0.0207
$\chi^2_{\text{d.o.f.}}$		28.29	11.60

([a]) Parameters of the physical baryon trajectories from eqs. (16)-(18). ([b]) The coefficient norm is chosen in such a way as to keep $A_{N_1^*} = 1$ in order to see the interplay between different resonances.

Thus, the "effective" SF becomes a function of some corrected trajectories $F(\alpha + \delta\alpha, x, Q^2)$, where α represents the physical value and $\delta\alpha$ the correction that takes account of subleading resonances. However, due to the fact that the physical resonances give dominant contribution, we expect this deviation to be not large.

In the light of these considerations, we have refitted the data, allowing the baryon-trajectory parameters to vary. The resulting parameters of such a fit are reported in table 1 (fourth column). It is worth noting that although the range of variation was not restricted, the new parameters of the trajectories remain close to their physical values, showing stability of the fit and thus reinforcing our previous considerations. From the relevant plots, shown in fig. 4 by full lines, one can see that the improvement is significant, although agreement is still far from being perfect ($\chi^2_{\text{d.o.f.}} = 11.6$).

Another important ingredient to be introduced in the model is spin. This changes the form factors in a nontrivial way, thus complicating the Q^2-dependence of the SFs (see ref. [29] for a recent treatment of the problem). These corrections have not yet been included in our study and might be responsible for relatively poor agreement with

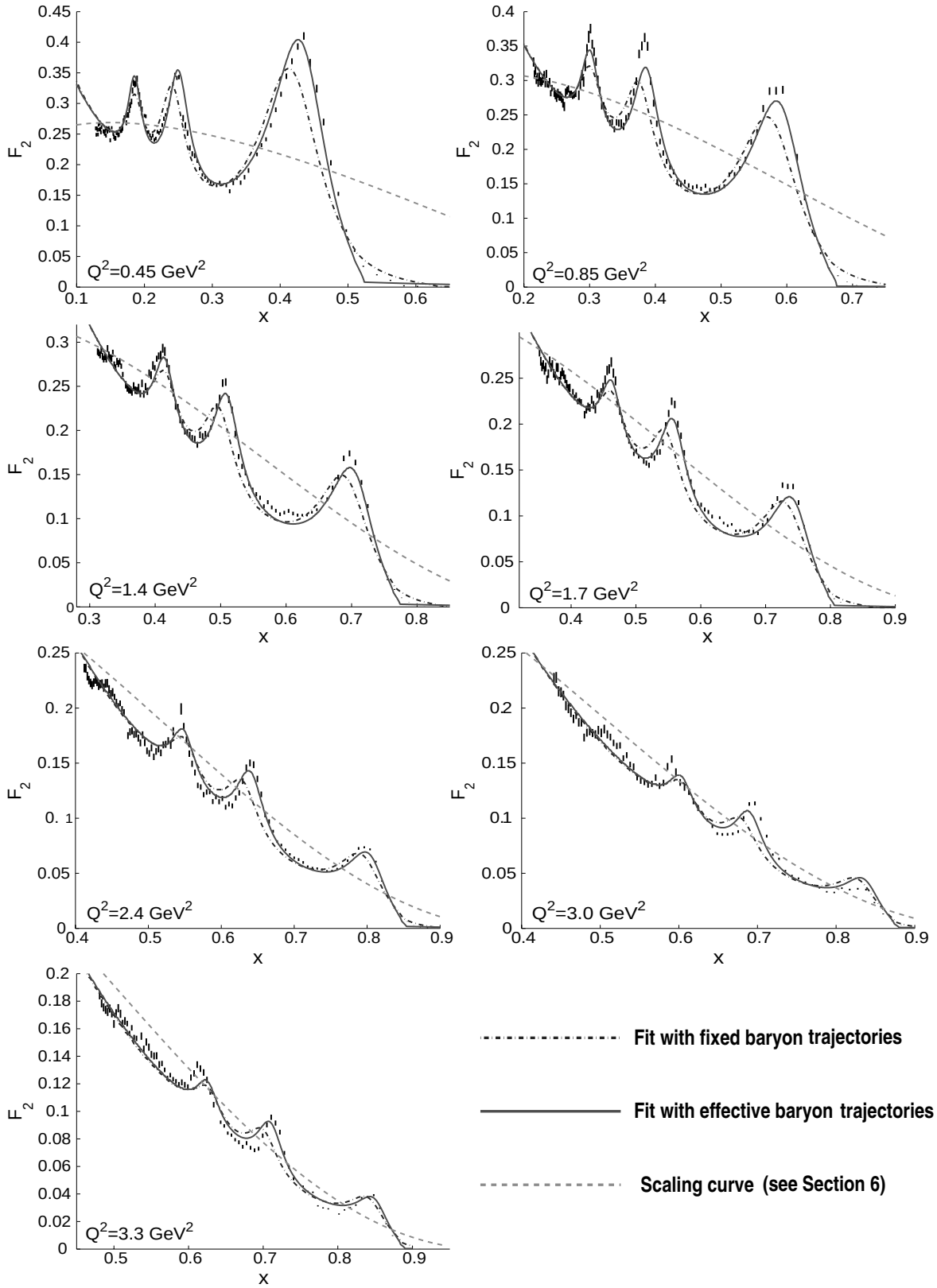

Fig. 4. F_2 as a function of x for $Q^2 = 0.45$–$3.3\,\mathrm{GeV}^2$.

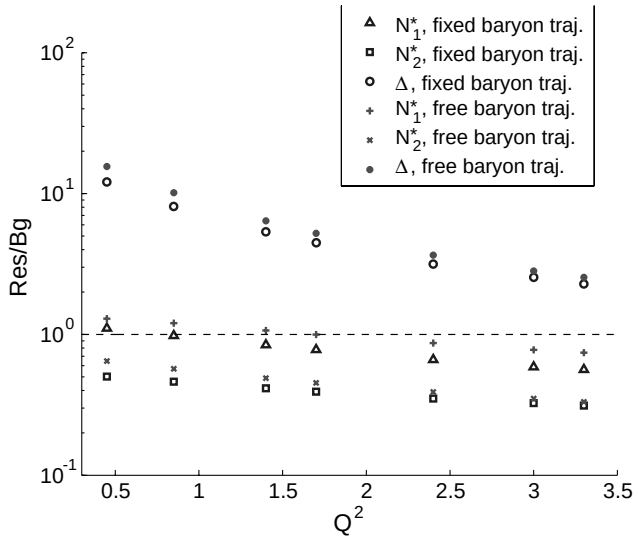

Fig. 5. The ratio of the resonance to background components of the SF at the resonance peaks. See text for more details.

data. We hope to address this problem in a forthcoming work.

One may also ask the question whether the dipole expression for the form factors of eq. (21) does work. To answer this question we performed the fit letting the powers of the $1/(1+Q^2/Q^2_{0,i})$ in eq. (21) free to vary. The results show that the second power is a good approximation —powers change only by about 5%. As we see in the next section, the dipole approximation deteriorates towards large values of Q^2. This phenomenon may be partly due to the spin effects ignored in the present model.

We have calculated also the Q^2-dependent ratio of the resonance to background components of the SF at three fixed values x, namely at three physical resonance peaks, $s_{N_1^*}$, $s_{N_2^*}$, s_Δ, for the fit with fixed physical baryon trajectories and at effective resonance peaks, $s^{\rm eff}_{N_1^*} = 1.494^2\,{\rm GeV}^2$, $s^{\rm eff}_{N_2^*} = 1.690^2\ {\rm GeV}^2$, $s^{\rm eff}_\Delta = 1.22^2\ {\rm GeV}^2$, for the fit with free baryon trajectories[3]. On this plot, the "background" for the selected resonance consists of three parts, *i.e.* contribution from the exotic trajectory (usual background term) and contributions from the two other resonances. The results are shown in fig. 5. One may see that for N_2^* and for N_1^* for $Q^2 > 1.5$ GeV^2 the "background" contributes more than the resonant term itself.

6 Parton-hadron duality: numerical tests

In order to check the validity of the quark-hadron duality, it would be helpful (see, *e.g.*, ref. [8]) to compare the Q^2-behaviour of the following quantities:

$$I_{\rm Bj}(Q^2) = \int_{s_{\rm th}}^{s_{\rm max}} {\rm d}s\ F_2^{\rm Bj}\ , \tag{22}$$

$$I_{\rm Model}(Q^2) = \int_{s_{\rm th}}^{s_{\rm max}} {\rm d}s\ F_2^{\rm Model}\ , \tag{23}$$

where the lower integration limit is fixed to $s_{\rm th} = s_0$ and the upper integration limit, $s_{\rm max}$, is varied within the range 3–25 GeV^2.

Here $F_2^{\rm Model}$ is our model, given by eqs. (9), (10), (15) and $F_2^{\rm Bj}$ is a "scaling curve", *i.e.* phenomenological parameterizations of the SF exhibiting Bjorken scaling and fitting to the data. We have chosen the parameterizations studied in ref. [31], which we report for the convenience of the reader,

$$F_2^{\rm Bj}(x,Q^2) = F_{\rm S}(x,Q^2) + F_{\rm NS}(x,Q^2)\ , \tag{24}$$

where

$$F_{\rm NS}(x,Q^2) = D\cdot x^{1-\alpha_{\rm R}}\cdot(1-x)^{n(Q^2)}\cdot\left(\frac{Q^2}{Q^2+b}\right)^{\alpha_{\rm R}}\ , \tag{25}$$

$$n(Q^2) = \frac{3}{2}\cdot\left(1+\frac{Q^2}{Q^2+c}\right)\ . \tag{26}$$

The singlet component of the SF, corresponding to a multipole (single+double+triple) Pomeron is a sum of logarithms

$$F_{\rm S}(x,Q^2) = Q^2\left[A\left(\frac{a}{a+Q^2}\right)^\alpha + B\left(\frac{a}{a+Q^2}\right)^\beta \log\left(\frac{Q^2}{x}\right) + C\left(\frac{a}{a+Q^2}\right)^\gamma \log^2\left(\frac{Q^2}{x}\right)\right](1-x)^{n(Q^2)+4}\ . \tag{27}$$

The values of the parameters, A, B, C, D, a, b, c, α, β, γ and $\alpha_{\rm R}$ can be found in [31]. Corresponding curves are presented by the dashed lines in fig. 4.

The quantity of interest is the so-called duality ratio given by

$$\mathcal{I}(Q^2) = \frac{I_{\rm Model}(Q^2)}{I_{\rm Bj}(Q^2)}\ . \tag{28}$$

Its deviation from the unity is an indication of any violation of the parton-hadron duality. We compute numerically this quantity, using values of the second set of parameters (table 1, fourth column) and show the result in fig. 6.

One can see from fig. 6 that for a short interval of integration our model strongly overshoots the "scaling curve", since in this region we have strongly peaked resonances. For $s_{\rm max}$ larger than 5 GeV^2 this effect saturates. As we tend to the large Q^2 region our model starts to underestimate the "scaling curve". It was stressed in ref. [31] that the scaling curve itself starts to overestimate the data for $Q^2 > 15$–20 GeV^2. The strong decrease of $\mathcal{I}(Q^2)$ for high Q^2 is partly due to this fact. The subplot shows that in the Q^2 interval of interest the $\mathcal{I}(Q^2)$ deviates from 1 by 20–40%.

[3] Note that the position of the N_2^*-resonance remains the same for the effective trajectory. Others also do not change much.

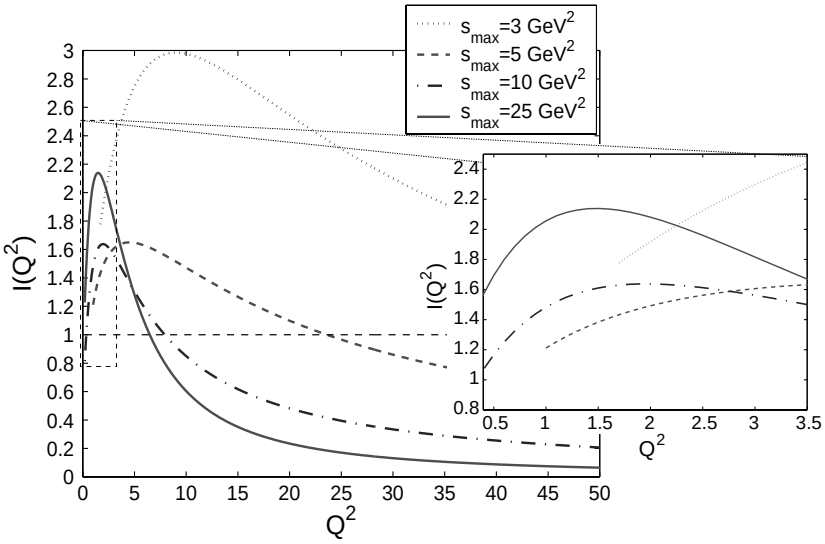

Fig. 6. Parton-hadron duality test for different $s_{\max}$.

7 Parton-hadron duality: analytical tests

Consider now the behaviour of $F_2(x,Q^2)$ at large x when s is kept in the resonance region. Recall that x, Q^2 and s are related by eq. (11) with $m = m_p$. Thus, each term in the rhs of eq. (15), using eqs. (9),(10) looks like

$$F_2(x,Q^2)_{i,n} = \frac{Q^2(1-x)}{4\pi\alpha\left(1+\frac{4m_p^2x^2}{Q^2}\right)} \frac{\text{norm } A_i}{\left(1+\frac{Q^2}{Q_{0,i}^2}\right)^{4(n-n_i^{\min}+1)}} \times \frac{\mathcal{I}m\ \alpha_i(s)}{(n-\mathcal{R}e\ \alpha_i(s))^2+(\mathcal{I}m\ \alpha_i(s))^2}\ . \quad (29)$$

In our case, since we consider only one resonance on each trajectory, we have

$$F_2(x,Q^2)_{i,n} \propto \frac{1}{\left(1+\frac{Q^2}{Q_{0,i}^2}\right)^4}\ . \quad (30)$$

In the limit of x going to 1 and s in the resonance region (1–4 GeV^2), $Q^2 = x(s-m_p^2)/(1-x)$ is much larger than s and $Q_{0,i}^2$, which are of the same order. Therefore,

$$\frac{1}{\left(1+\frac{Q^2}{Q_{0,i}^2}\right)^4} \approx \frac{(1-x)^4}{\left(\frac{x(s-m_p^2)}{Q_{0,i}^2}\right)^4}\left(1-4\frac{Q_{0,i}^2}{Q^2}+O\left(\frac{1}{Q^4}\right)\right)\ . \quad (31)$$

Using $x = Q^2/(Q^2+s-m_p^2) = 1-(s-m_p^2)/Q^2$ we can go one step further

$$\frac{1}{\left(1+\frac{Q^2}{Q_{0,i}^2}\right)^4} \approx \frac{(1-x)^4}{\left(\frac{(s-m_p^2)}{Q_{0,i}^2}\right)^4} \times\left(1-4\frac{Q_{0,i}^2+s-m_p^2}{Q^2}+O\left(\frac{1}{Q^4}\right)\right). \quad (32)$$

Thus,

$$F_2(x,Q^2) \approx \text{norm} \sum_{i=N_1^*,N_2^*,\Delta,E} A_i \sum_{n=n_i^{\min}}^{n_i^{\max}} (1-x)^4 \times M_{i,n}(x,Q^2)\left(1-4\frac{Q_{0,i}^2+s-m_p^2}{Q^2}+O\left(\frac{1}{Q^4}\right)\right), \quad (33)$$

where

$$M_{i,n}(x,Q^2) = \frac{(s-m_p^2)x}{4\pi\alpha\left(1+\frac{4m_p^2x^2}{Q^2}\right)}\left(\frac{Q_{0,i}^2}{s-m_p^2}\right)^4 \times \frac{\mathcal{I}m\ \alpha_i(s)}{(n-\mathcal{R}e\ \alpha_i(s))^2+(\mathcal{I}m\ \alpha_i(s))^2}\ . \quad (34)$$

In the range of our interest, $M_{i,n}$ is a slowly varying function of both x and Q^2. For each (i,n) the term proportional to $(1-x)^{4(n-n_i^{\max}+1)}$ shows the main tendency of $F_2(x,Q^2)_{i,n}$, while $M_{i,n}$ is responsible for the "fine structure" —resonances at large x. Of course, for each trajectory i the main contribution comes from the first resonance —$(1-x)^4$.

At this point it might be interesting to see the effect of spin corrections. As was shown in ref. [29], if one explicitly takes into account the spin structure of the F_2, the main contribution from each resonance in the limit $x \to 1$ ($Q^2 \to \infty$) is proportional to $(1-x)^3$. Thus our model, with spin effects being neglected, strongly underestimate the physical SF. This might be another reason why the duality ratio, eq. (28), is so small in the high-Q^2 region.

8 Conclusions

The idea of the present paper is that deep-inelastic scattering can be described by a sum of direct channel resonances

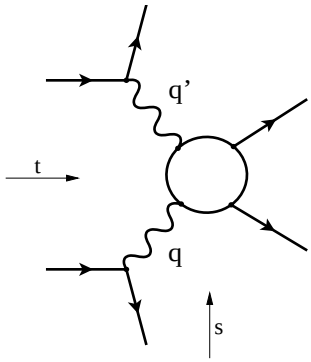

Fig. 7. Typical six-point function ansatz.

lying on Regge trajectories. The form of these trajectories is crucial for the dynamics. It is constrained by analyticity, unitarity and by the experimental data. The use of baryon trajectories instead of individual resonances not only makes the model economic (several resonances are replaced by one trajectory) but also helps in classifying the resonances, by including the "right" ones and eliminating those nonexistent.

Compton scattering of nuclei is much similar to πN scattering. The difference coming mainly from the photon spin imposes selection rules on inelastic transitions. These selection rules are approximate, and can be introduced either in the construction of the scattering amplitude (cross-section, SF), or just by fitting the model to the data.

To fix the ideas and make a rough fit to the data, we constructed a simplified model with just 3 baryon trajectories, in which heavy thresholds have been replaced for simplicity by a linear term, and with the lowest-lying resonances. In fact, apart from the "prominent" three resonances many more should be included by means of relevant baryon trajectories. To this end an independent study of baryon trajectories and updated fits to dozens of existing resonances should be done. We intend to continue working in this direction.

The dynamics of DIS can be described either by the contribution of direct-channel or cross-channel Regge trajectories.

An important issue of our paper is the integral representation realizing parton-hadron, or Bloom-Gilman duality. This can be seen from the equivalence of its pole decomposition (resonances) and smooth large-Q^2 scaling behaviour. As a result, a Q^2-dependent photon Regge trajectory emerges. In the unphysical region of positive q^2 (negative Q^2), outside the one we consider, resonances are expected to appear on this trajectory. As it is known, these are the vector mesons $\rho, \omega, \phi, J/\Psi$, etc. The nonappearance of higher recurrences, with spin larger than 1, on the photon trajectory is a problem for linear photon trajectories. "Analytical" models of Regge trajectories used in our paper can resolve this problem: the real part of the photon trajectory is limited by $\mathcal{R}e\ \alpha_\gamma(Q^2) < 2$ and higher than spin one states are not expected there.

The dual model presented here is a part of a more general 6-point dual amplitude (see fig. 7), where two pairs of external particles (electrons) are at a pole, corresponding to the photon trajectory $\alpha_\gamma(Q^2)$. Such a dual model, but without the important limitation $\mathcal{R}e\ \alpha_\gamma(Q^2) < 2$ and for $t = 0$, was considered in ref. [32]. Relaxing the condition $t = 0$ one can apply the 6-point dual amplitude with the above trajectories to DIS in all possible kinematical regions, including off-diagonal or skew-symmetric (*i.e.* where $t \neq 0$) DIS. We intend to report on relevant results in a forthcoming publication.

We thank F. Paccanoni, E. Predazzi and B.V. Struminsky for fruitful discussions and I. Niculescu for a very useful and stimulating correspondence. L.J. and V.M. acknowledge the support from INTAS, grant 00-00366. Work is also supported in part by the Ministero dell'Istruzione, dell'Università e della Ricerca (MIUR). A.F. and V.M. wish to thank the University of Calabria, where this work was completed, for the warm hospitality. A.F. is supported by the EU-Marie Curie post doctoral fellowship program.

References

1. M. Köbberling *et al.*, Nucl. Phys. **82**, 201 (1974).
2. S. Stein *et al.*, Phys. Rev. **12**, 1884 (1975).
3. F.W. Brasse *et al.*, Nucl. Phys. B **110**, 413 (1976).
4. A. Bodek *et al.*, Phys. Rev. D **20**, 1471 (1979).
5. L.J. Whitlow *et al.*, Phys. Lett. B **250**, 193 (1990).
6. T.H. Bauer *et al.*, Rev. Mod. Phys. **50**, 261 (1978).
7. P. Stoler, Phys. Rev. D **44**, 73 (1991); Phys. Rev. Lett. **66**, 1003 (1991).
8. I. Niculescu, PhD Thesis, Hampton University, May 1999.
9. C.E. Carlson, N.C. Mukhopadhyaya, Phys. Rev. Lett. **74**, 1288 (1995); Phys. Rev. D **58**, 094029 (1998).
10. C.E. Carlson, J.L. Poor, Phys. Rev. D **38**, 2758 (1988); X. Ji, P. Unrau, Phys. Rev. D **52**, 72 (1995).
11. G. Sterman, P. Stoler, Annu. Rev. Nucl. Part. Sci. **47**, 193 (1997).
12. C.E Carlson, N.C. Mukhopadhyay, Phys. Rev. D **58**, 094029 (1998); X. Ji, W. Melnitchouk, Phys. Rev. D **56**, 1 (1997); D. Qing, I. Schmidt, hep-ph/0106225; V.D. Burkert, nucl-ex/0108023, nucl-ex/0109004.
13. I. Niculescu *et al.*, Phys. Rev. Lett. **85**, 1182; 1186 (2000).
14. C.S. Armstrong *et al.*, hep-ph/0104055.
15. R. Ent, C.E. Koppel, I. Niculescu, Phys. Rev. D **62**, 073008 (2000).
16. S. Simula, Phys. Lett. B **481**, 14 (2000).
17. L.L. Jenkovszky, V.K. Magas, E. Predazzi, Eur. Phys. J. A **12**, 361 (2001).
18. L.L. Jenkovszky, V.K. Magas, E. Predazzi, nucl-th/0110085; L.L. Jenkovszky, V.K. Magas, in *Proceedings of the 31st International Symposium On Multiparticle Dynamics (ISMD 2001), September 1-7, 2001, Datong, China*, edited by B. Yuting, Yu Meiling, Wu Yuanfang (World Scientific, 2002) p. 74, hep-ph/0111398; L.L. Jenkovszky, T. Korzhinskaja, V.I. Kuvshinov, V.K. Magas, in *Proceedings of the New Trend in High-Energy Physics, Yalta, Crimea, Ukraine, September 22-29, 2001*, edited by P.N. Bogolyubov, L.L. Jenkovszky (Bogolyubov Institute for Theoretical Physics, Kiev, 2001) p. 178.

19. L.L. Jenkovszky, V.K. Magas, T. Szabo, in *Proceedings of the International Worshop on Very High Mulitiplicities, Dubna, Russia, 7-9 April 2001* (Dubna, JINR, 2002) p. 185.
20. R. Fiore, L. Jenkovszky, V. Magas, F. Paccanoni, A. Papa, Eur. Phys. J. A **10**, 217 (2001); Nucl. Phys. Proc. Suppl. **99**, 68 (2001).
21. P. Freund, Phys. Rev. Lett. **20**, 235 (1968); H. Harari, Phys. Rev. Lett. **20**, 1395 (1968).
22. G. Domokos, S. Kövesi-Domokos, E. Schoenberg, Phys. Rev. **3**, 1184 (1971).
23. F. Halzen, A.D. Martin, *Quarks & Leptons: An Introductory Course in Modern Particle Physics* (John Wiley & Sons, 1984); F.E. Close, *An Introduction to Quarks and Partons* (Academic Press, 1979).
24. P.D.B. Collins, *Introduction to Regge Theory and High Energy Physics* (University Press, 1977).
25. A.V. Anisovich, V.V. Anisovich, A.V. Sarantsev, Phys. Rev. D **62**, 051502 (2000).
26. A. Bugrij *et al.*, Fortschr. Phys. **21**, 427 (1973).
27. V. Magas, Ukr. Fiz. Zh. **44**, 438 (1999); R. Fiore, L.L. Jenkovszky, V.K. Magas, F. Paccanoni, Phys. Rev. D **60**, 116003 (1999).
28. Particle Data Group, Eur. Phys. J. C **3**, 1 (1998).
29. V.V. Davydovsky, B.V. Struminsky, hep-ph/0205130.
30. `http://www.jlab.org/resdata.`
31. L. Csernai, L. Jenkovszky, K. Kontros, A. Lengyel, V. Magas, F. Paccanoni, Eur. Phys. J. C **24**, 205 (2002).
32. F. Schierholz, M.G. Schmidt, Phys. Rev. D **10**, 175 (1974).